Korea-Australia Rheology Journal
Vol. 11, No. 3, September 1999 pp.247-253

Study on the growth of vapor bubble in devolatilization of polymers

Chongyoup Kim*
Department of Polymer Engineering Chungnam National University
220 Goong-dong, Yoosong-goo Taejeon 305-764, Korea
(Received June 24, 1999; final revision received July 14, 1999)

Abstract

The growth of a spherical vapor bubble contained in a large body of upper convected Maxwell fluid is theoretically analyzed under the devolatilization condition of polymer by using a Galerkin FEM in the Lagrangian frame. Using the finite element technique, a fully explicit numerical scheme is developed both for the calculation of pressure distribution and for the tracking of bubble surface. Oscillatory behavior in bubble radius is observed during growth and the oscillatory behavior is found to be due to the interaction of mass transfer resistance and elasticity. It is found that the elasticity of fluid accelerates the growth and removal of volatile component. It is also found that the bubble growth in the devolatilization of polymers is affected by both mass transfer resistance and viscoelasticity of fluids.

Key words : Lagrangian frame, elasticity, rebound, diffusion

1. Introduction

Polymer devolatilization is a separation process in which undesirable volatile components are removed from bulk polymers. The concentrations at which these volatiles are present may be as low as ppm or as high as tens of percent. Removal of these volatiles are performed for several reasons such as improvement of the properties of polymer, recovery of monomer or solvent, fulfillment of environmental regulations, elimination of odors or increase of the conversion of step-growth polymerization.

Devolatilization is carried out in various equipment. Sebastian and Biesenberger (1983) classified these equipment into two main categories: rotating devolatilizers and non-rotating devolatilizers. In a rotating devolatilizer such as vented extruders, bubbles containing vapor of the volatile material are nucleated, grow and finally burst. During the growth, the volatile component is vaporized into the bubble, hence the removal of volatile component is achieved. Therefore, the growth of bubble is one of the most crucial stages in the devolatilization process.

The growth of bubbles in non-Newtonian fluids has been the subject of several investigations in the past (Zana and Leal, 1975; Han and Yoo, 1981; Papanastasiou *et al.*, 1984; Favelukis and Albalak, 1996; Afremanesh and Advani, 1991). It has been reported that the rate of bubble growth is enhanced by elasticity of the polymeric liquid relative to the purely viscous case. Recently Venerus *et al.*(1998) formulated the problem rigorously by containing all the relevant terms such as viscoelasticity, inertia, surface tension and diffusion. They solved the problem without introducing any approximation technique such as the thin boundary layer approximation (TBLA) and the infinitely dilute solute approximation (IDSA) which have been used extensively in previous studies and showed that TBLA had a rather limited range of applicability. They also showed that IDSA was valid when the amount of volatile component was less than 10%. However, in solving the governing equations, they fixed several parameters that were related to viscosity, vapor pressure, inertia and surface tension. However, these terms are expected to play important roles in the growth of bubbles in most devolatilization processes. Therefore, in this paper we address the growth of a vapor bubble in viscoelastic polymeric liquids while keeping these terms in formulating and solving the problems.

The problem of bubble growth is a moving boundary problem in hydrodynamics in which the location of bubble surface and pressure should be determined. In numerical solutions, severe iterations are required to determine these two values. Therefore we adopt the finite element method in the Lagrangian reference frame (Kim, 1994) in which no iteration is required to determine the location of bubble boundary and hydrodynamic pressure.

In the next section the physical problem is formulated. In Section 3, the numerical method is described. In Section 4, parametric studies are described together with some results for more realistic devolatilization conditions. The result shows that the bubble growth is faster and mass transfer is enhanced in elastic liquids. It also shows that, during the growth, inertia is important in the

*Corresponding author: cykim@hanbat.chungnam.ac.kr

early stage of growth and bubbles oscillate as in the case of collapse process. However the oscillation is caused by the interaction of mass transfer and elasticity unlikely the case of collapse in which the oscillation is caused by inertia and elasticity.

2. Formulation of the problem

Let us consider a spherical vapor bubble of radius R_0 contained in a large body of incompressible polymeric liquid with a dissolved volatile component. Until the reference time $t_0 = 0$, the pressure is uniform at p_0 and the fluid is at rest. The concentration of volatile component is also uniform at C_0 until t_0 and the vapor inside the bubble is in the thermodynamic equilibrium with the volatile component in the liquid. At $t = 0$, the pressure far from the bubble is set to be zero. Then, due to the pressure difference between the fluid and bubble, the bubble begins to grow. As the bubble grows the pressure inside the bubble is reduced, hence the thermodynamic equilibrium is broken. Then the volatile component begins to vaporize at the bubble surface to result in the concentration gradient inside the liquid. Then the volatile component diffuses toward the bubble surface according to the Fick's law.

To treat this problem we need to solve the following conservation equations together with a constitutive equation for the polymeric liquid:

$$\rho\left(\frac{\partial \mathbf{v}}{\partial t}+\mathbf{v}\cdot\nabla\mathbf{v}\right)=-\nabla p+\nabla\cdot\tau \tag{1}$$

$$\nabla\cdot\mathbf{v}=0 \tag{2}$$

$$\frac{DC}{Dt}=D\nabla^2C \tag{3}$$

$$\frac{DT}{Dt}=\alpha\nabla^2T \tag{4}$$

In the above equation $\mathbf{v}$ is velocity, t is time, p is pressure, τ is stress, C is the concentration of the volatile material, D is mass diffusivity, T is temperature and α is thermal diffusivity. As the constitutive equation we choose the upper-convected Maxwell model:

$$\tau+\lambda\frac{\delta\tau}{\delta t}=2\eta\mathbf{D} \tag{5}$$

where $\delta/\delta t$ denotes the upper convected derivative and $\mathbf{D}$ is the rate of deformation tensor defined as follows:

$$\frac{\delta\tau}{\delta t}=\frac{D\tau}{Dt}-(\nabla\mathbf{v})^T\cdot\tau-\tau\cdot\nabla\mathbf{v} \tag{6}$$

$$\mathbf{D}=\frac{1}{2}[\nabla\mathbf{v}+(\nabla\mathbf{v})^T] \tag{7}$$

In solving the above equations, the following assumptions are introduced:

(i) There is no gravitational effect.
(ii) The motion is spherically symmetric.
(iii) The system is in an isothermal state.
(iv) The fluid is contained between the bubble boundary and an imaginary outer boundary of radius r_o on which no force is exerted during the growth.
(v) The vapor inside the bubble follows the ideal gas law.

Assumption (iii) can be introduced since the heat of vaporization to be supplied to the system usually has a negligible effect on the temperature profile at the low volatile concentrations at which devolatilization processes are often conducted. Therefore we shall leave out Eqn. (4) in the following.

The driving force for the growth of bubble is the pressure difference between the gas and the outer boundary. To determine the pressure inside the bubble, the principle of mass conservation is applied to the gas inside the bubble, which results in the following equation:

$$\frac{d}{dt}\left(\frac{4\pi}{3R_gT}P_BR^3\right)=4\pi R^2D\left.\frac{\partial C}{\partial r}\right|_{r=R} \tag{8}$$

where R_g is the gas constant and $(\partial C/\partial r)_{r=R}$ is the concentration gradient at the bubble wall. Rearrangement of Eqn. (8) yields

$$R\frac{dP_B}{dt}=-3P_B\frac{dR}{dt}+3R_gTD\left.\frac{\partial C}{\partial r}\right|_{r=R} \tag{9}$$

which is used as the evolution equation for the pressure inside the bubble. At $t = 0$, the system is in the equilibrium state. Thus the initial condition is

$$R = R_0,\ P_B = P_{B0} \tag{10,11}$$
$$C = C_0,\ \tau = 0,\ \mathbf{v} = 0 \text{ for } R_0 < r < r_o \tag{12,13,14}$$

At the bubble interface, the following relation is applied:

$$P_B - p + \tau_{rr} = \frac{2\sigma}{R} \tag{15}$$

$$P_B = K_wC \tag{16}$$

where at the bubble boundary the vapor in the bubble is in thermodynamic equilibrium with the liquid at the bubble boundary and Henry's law constant is K_w. At the outer boundary, r_o,

$$\frac{\partial C}{\partial r}=0 \tag{17}$$

$$f=-p+\tau_{rr}=0 \tag{18}$$

To solve the above problem with a time dependent free surface, it is advantageous to rewrite the equations in the Lagrangian frame of reference. This method was successfully applied to the collapse problem by Kim (1994). To be more readable the Lagrangian method is briefly explained in the following.

To transform the eqns. (1)-(3) to those in the Lagrangian

kinematic description, the coordinate **x** should be a dependent variable while the fluid particle label becomes an independent variable. It is usual to specify the particle label as the coordinate $\mathbf{x}^0$ at the reference time t_0. Thus the fluid particle label and displacement function **x** are related as follows:

$$\mathbf{x} = \mathbf{x}\ (\mathbf{x}^0,\ t_0,\ t) \tag{19}$$

This relation refers to a mapping on **x** at time t of the material point which at the reference time t_0 occupies the position given by the reference coordinates $\mathbf{x}^0$. Other de- pendent variables are Lagrangian velocity $\mathbf{u} = \mathbf{u}\ (\mathbf{x}^0, t_0, t)$, Lagrangian concentration $C = C\ (\mathbf{x}^0,\ t_0,\ t)$ and Lagrangian pressure $p = p(\mathbf{x}^0, t_0, t)$. If we replace these Lagrangian variables with the Eulerian variables in eqns. (1)-(3), we obtain the governing equations in the Lagrangian frame of reference. The equation of continuity also can be written in terms of deformation gradient $\mathbf{E} = \partial\mathbf{x}/\partial\mathbf{x}'$. For incompress- ible fluids, it is found to be more convenient to use the relationship

$$a = \det\ \mathbf{E} = 1 \tag{20}$$

when seeking numerical solutions. In the constitutive equation (5), we replace the material derivative and velocity gradient with the Lagrangian derivative and derivative with respect to fluid particle label, respectively. Then we finally obtain the governing equations in the Lagrangian frame as follows:

$$\rho\frac{d\mathbf{v}}{dt} = -\nabla p + \nabla\cdot\tau \tag{21}$$

$$\det\ \mathbf{E} = 1 \tag{22}$$

$$\frac{d\mathbf{x}}{dt} = \mathbf{v} \tag{23}$$

$$\tau + \lambda\frac{\delta\tau}{\delta t} = 2\eta\ \mathbf{D} \tag{24}$$

$$\frac{dC}{dt} = D(\nabla\cdot\nabla C) \tag{25}$$

where the time derivative d/dt represents the Lagrangian time derivative and ∇ represents the gradient operator with respect to material point. The upper convected derivative and rate of deformation tensor in eqn. (25) also should be expressed in terms of the Lagrangian variables correspondingly.

For spherically symmetric deformations, the deformation gradient **E** and the rate of deformation tensor **D** are diagonal. The stress tensor is also diagonal and

$$\tau_{\theta\theta} = \tau_{\phi\phi} \tag{26}$$

Therefore, the equation of motion, continuity equation and the constitutive equation can be written as follows:

$$\rho\frac{du_r}{dt} = -\frac{\partial p}{\partial r} + \frac{1}{r^2}\frac{\partial}{\partial r}(r^2\tau_{rr}) - \frac{2\tau_{\theta\theta}}{r} \tag{27}$$

$$\left(\frac{\partial r}{\partial r'}\right)\left(\frac{r}{r'}\right)^2 = 1 \tag{28}$$

$$\tau_{rr} + \lambda\left(\frac{d\tau_{rr}}{dt} - 2\tau_{rr}\frac{\partial u_r}{\partial r}\right) = 2\eta\frac{\partial u_r}{\partial r} \tag{29}$$

$$\tau_{\theta\theta} + \lambda\left(\frac{d\tau_{\theta\theta}}{dt} - 2\tau_{\theta\theta}\frac{u_r}{r}\right) = 2\eta\frac{u_r}{r} \tag{30}$$

$$\frac{dC}{dt} = D\frac{1}{r^2}\frac{\partial}{\partial r}\left(r^2\frac{\partial C}{\partial r}\right) \tag{31}$$

Eqns. (27)-(31) are made dimensionless using the length and time scales of the intial radius R_0, the initial concentration C_0 and the Rayleigh time scale $T_R = (\rho/p_0)^{1/2}R_0$ respectively. Then, the non-dimensionalized governing equations are

$$\frac{du}{dt} = -\frac{\partial p}{\partial r} + \frac{\partial\tau_1}{\partial r} + 2\left(\frac{\tau_1}{r} - \frac{\tau_2}{r}\right) \tag{32}$$

$$\frac{dr}{dt} = u \tag{33}$$

$$\left(\frac{\partial r}{\partial r'}\right)\left(\frac{r}{r'}\right)^2 = 1 \tag{34}$$

$$\tau_1 + De\left(\frac{d\tau_1}{dt} - 2\tau_1\frac{\partial u}{\partial r}\right) = \frac{2}{Re}\frac{\partial u}{\partial r} \tag{35}$$

$$\tau_2 + De\left(\frac{d\tau_2}{dt} - 2\tau_2\frac{u}{r}\right) = \frac{2}{Re}\frac{u}{r} \tag{36}$$

$$\frac{dx}{dt} = \beta\frac{1}{r^2}\frac{\partial}{\partial r}\left(r^2\frac{\partial x}{\partial r}\right) \tag{37}$$

where $x = C/C_0$, $\tau_1 = \tau_{rr}/p_0$, and $\tau_2 = \tau_{\theta\theta}/p_0$. Also we have used the same notation for dimensionless variables as the corresponding dimensioned variables when there arises no confusion. Eqn. (9) also can be written in the dimensionless form as follows:

$$\frac{dy}{dt} = -3y\frac{1}{R}\frac{dR}{dt} + 3\beta\gamma\frac{1}{R}\frac{\partial x}{\partial r}\bigg|_{r=R} \tag{38}$$

where $y = P_B/P_{B0}$. The equilibrium at the bubble surface can be written as follows:

$$f = -p + \tau - We\frac{1}{r} \tag{39}$$

In the above equations, we have introduced the following dimensionless groups :

Reynolds number : $Re = R_0(\rho p_0)^{1/2}/\eta$ (40)

Deborah number : $De = \lambda/(\rho R_0^2/p_0)^{1/2}$ (41)

Dimensionless diffusivity : $\beta = D(\rho R_0^2/p_0)^{1/2}/R_0^2$ (42)

Foam number : $\gamma = R_g T_0 C_0/p_0$ (43)

Weber number : $We = 2\sigma/R_0 p_0$ (44)

The initial conditions at t = 0 are

$$P_B = 1,\ R_0 = 1,\ u = 0,\ x = 1,\ \tau_1 = 0,\ \tau_2 = 0 \tag{45-50}$$

To solve the eqns. (32)-(38), the Galerkin-finite element method is used. The detailed derivation can be found in Kim(1994). The initial nodal positions are listed in Table 1.

3. Results and Discussion

The growth process is controlled by many different variables and parameters such as viscosity, relaxation time, diffusion coefficient, vapor pressure, surface tension and initial bubble radius. The influence of these physical variables can be analyzed by varying the corresponding dimensionless parameters listed in Eqns. (40)-(44). In this paper we focused on the effect of viscoelasticity, diffusion and vapor pressure of the polymeric liquid on growth process. The values of the reference parameters selected here are typical of a devolatilization process. Specifically we basically refer to the devolatilization of styrene from the mixture of polystyrene and styrene even though we do not try to simulate the system at a specific condition. In Table 2, a typical operating condition for devolatilization is shown together with the corresponding dimensionless parameters for differing bubble radius. In the following we examine the effect of relevant variables by varying one of the dimensionless groups.

3.1 Effect of inertia

In Fig. 1, the effect of Reynolds number is shown with the Deborah number fixed at 10. As the Reynolds number becomes larger, in other words, as the viscosity is smaller or the initial bubble radius is larger, the bubble grows faster. This is what we expect normally. However we can notice in the figure that the oscillation characteristics is not monotonic as the Reynolds number increases from 0.01 to 1.0. In the case of collapse, as Reynolds number increases, the oscillation becomes more conspicuous indicating that the oscillation is caused by the interaction of inertia and elasticity (Kim, 1994). The non-monotonicity with Re suggests that the oscillation of bubble radius during the growth process should not be caused by the inertial effect. The mechanism of oscillation will be discussed further in the following section.

When we examine the effect of Reynolds number in relation to the devolatilization process, we may find that initially larger bubbles grow faster than smaller bubbles. This means that the rate of devolatilization is dependent on the size of nucleus as well as the rate of nucleation. Also, once small bubbles get coalesced, the larger bubble grows with a more accelerated velocity. Hence it is surmised that the bubble coalescence in the shear field plays an important role in devolatilization.

Table 1. Initial nodal positions used in FEM.

Node Number	Nodal Position
1	1.0
2	1.02
3	1.05
4	1.1
5	1.2
6	1.3
7	1.5
8	1.75
9	2.0
10	2.5
11	3.5
12	5.0
13	10.0
14	100.0
15	1000.0

Table 2. A typical set of devolatilization condition for polystyrene-styrene system and corresponding dimensionless groups.

Devolatilization Condition[a]	
Temperature	533 K
Solvent fraction	0.01
Polymer fraction	0.99
Molecular weight	280,000 g/mol
D_1[b]	.11312E-04 cm^2/sec
Diffusivity, D[b]	.11036E-04 cm^2/sec
K_w[c]	40.18674 atm
σ[c]	7.77722 N/m
Density[c]	.66310 g/cm^3
Viscosity[d]	50346.99 Pa.s
Relaxation time[e]	.53296 sec
Solvent concentration	63.76 kg/m^3

Dimensioles Number	When $R_0 = 1\mu$	When $R_0 = 10\mu$	When $R_0 = 100\mu$	When $R_0 = 1000\mu$
Re	.10319E-05	.10319E-04	.10319E-03	.10319E-02
De	.41756E+08	.41756E+07	.41756E+06	.41756E+05
We	.38214E-02	.38214E-03	.38214E-04	.38214E-05
β	.14086E-04	.14086E-05	.14086E-06	.14086E-07
γ	.69414E-01	.69414E-01	.69414E-01	.69414E-01

a) Biesenberger (1983)
b) Estimated using the method suggested by Duda *et al*(1982).
c) Albalak (1996)
d) Mendelson (1979, 1980)
e) Estimated by Doi-Edwards theory(Doi and Edwards, 1986)

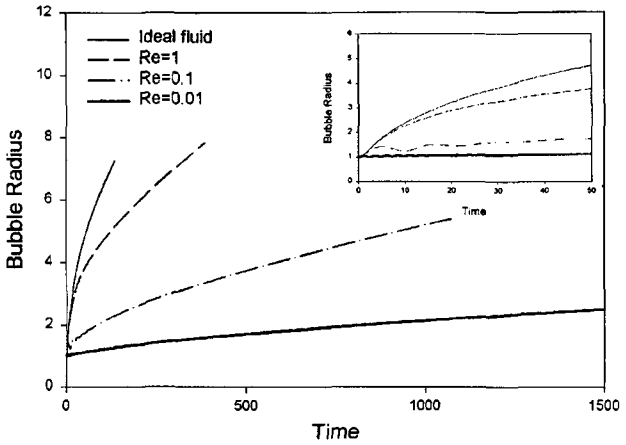

Fig. 1. The effect of Reynolds number on bubble growth when De = 10, We = 0, $\beta = 10^{-5}$ and $\gamma = 1$. The box in the figure shows the magnified view at the initial stage.

3.2 Effect of Elasticity

To examine the effect of elasticity, the growth curves are shown in Fig. 2 for differing De when Re is fixed. The growth rate is the slowest in Newtonian fluid and the fastest in the perfect fluid. In viscoelastic fluid, the growth rate stays between these two extreme values. This means that the elasticity of fluid accelerates the growth rate in viscoelastic fluids. This is because the viscoelastic stress has not been developed yet at the initial stage of the growth.

In the figure we notice that oscillatory motions are observed during growth. We may argue that the oscillation of bubble radius is caused by the following mechanism: When the Deborah number is large, the viscoelastic stress remains small in the initial stage of growth because it takes time to develop to a large value. Therefore the bubble grows very fast as if it resides in an ideal fluid. As the bubble grows, the bubble pressure drops off rapidly. Also the velocity and velocity gradient become very large to result

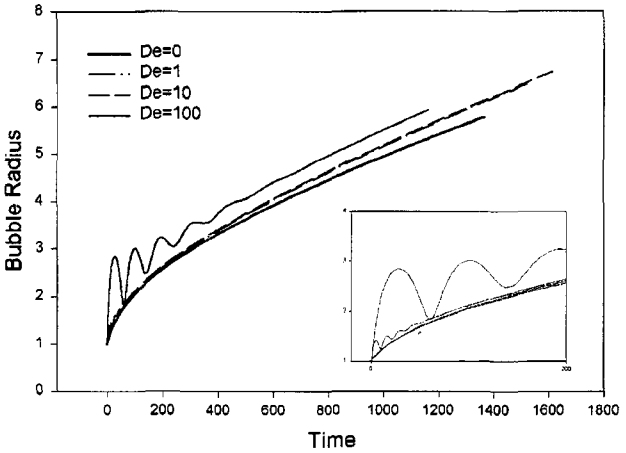

Fig. 2. The effect of Deborah number on bubble growth when Re = 0.1, We = 0, $\beta = 10^{-5}$ and $\gamma = 1$. The box in the figure shows the magnified view at the initial stage.

in large viscoelastic stresses. When the bubble grows sufficiently large, the force to expand the bubble (i.e., pressure) and the force to suppress the growth(i.e., viscoelastic stress) get balanced. After this point the bubble pressure cannot overcome the viscoelastic stress, hence the bubble begins to collapse. As the bubble continues to collapse, the bubble pressure increases and the viscoelastic stress decreases. When the bubble pressure and viscoelastic stress are balanced the bubble grows again. As the growth and collapse alternate, the oscillation becomes weak due to viscous dissipation. As time passes, the amount of volatile component in the bubble increases due to diffusion and hence the bubble grows in the average sense while it oscillates. Therefore the oscillation we observe here is caused by the interaction of diffusion and viscoelasticity unlikely the case of collapse in which the oscillation is caused by the interaction of inertia and viscoelasticity.

The rate of mass transfer is accelerated due to the oscillation. When the Deborah number is 100, the growth rate is larger compared with the other cases. It appears that the driving force of diffusion becomes large at the bubble interface due to the low value of pressure when the bubble grows rapidly. When the oscillatory motion is dissipated, the growth rate shows almost no difference.

To the author's knowledge, this is the first report on the oscillation of bubble during growth. Venerus and Yala (1998) recently reported a systematic study on bubble growth. In deriving the non-dimensional governing equations, they used the diffusion time ($T_D = R^2/D$, approximately 1 second) as the reference time scale which has orders of magnitude larger than the Rayleigh's inertial time scale (approximately 1 millisecond) used in this research. This may be one of the reasons why they were not able to observe any oscillations during the initial stage of growth. Since the Rayleigh time scale is much shorter than the diffusion time scale, the Rayleigh time scale should be more appropriate to examine the short time behavior when inertial effect is included. Venerus and Yala used the initial liquid pressure as the initial bubble pressure. In this case the initial growth rate appears to be too small to develop sufficiently large viscoelastic stress to overcome the bubble pressure and hence they do not observe the rebound of bubble radius.

3.3 Effect of diffusion coefficient

The bubble growth is directly affected by the diffusion coefficient. When the diffusion is rate controlling, the radius of bubble scales as the square root of diffusivity. When viscoelasticity or inertia are included, the growth will be less sensitive to diffusivity. In Fig. 3, growth curves are shown for differing $\beta = DT_0/R_0^2$. In the early stage of growth, the growth is almost independent of β. This is because the vapor is abundant near the bubble surface and hence the diffusion resistance is not severe compared with inertia or vis-

coelasticity. As the bubble grows, the vapor near the surface diminishes and the diffusional resistance becomes larger when β is small. In Fig. 4, the bubble radius is plotted against $(\beta t)^{1/2}$. When the bubble growth is strictly diffusion-controlled, all the curves will fall on the same curve for differing β. But it is noticed that the growth rate is smaller for larger β. This means that the viscoelasticity cannot be neglected even in the later stage of growth when the influence of diffusion resistance becomes more important.

3.4 Effect of Vapor Pressure

Vapor pressure is the driving force of growth. Vapor pressure can be expressed by the Henry's law and the relevant dimensionless parameter is the Foam number. In Fig. 5, growth curves are shown for differing foam number. In the early stage of growth, the growth is almost independent of foam number. The is because the bubble is filled with the vapor initially. As the bubble grows, the pressure decrea- ses. If the vapor pressure is small, the vapor supply is limited, hence the growth rate decreases faster. Scriven(1959) has shown that, when the viscous force is neglected, the radius of bubble can be written as follows:

$$\text{Small } \gamma : R(t) = \sqrt{2\gamma Dt} \quad (51)$$

$$\text{Large } \gamma : R(t) = \sqrt{12Dt/\pi}\,\gamma \quad (52)$$

In Fig. 6 and 7, bubble radius is plotted against $\gamma t^{1/2}$ and $(\gamma t)^{1/2}$. If the bubble growth is controlled by diffusion and the supply of the volatile component, the growth curves should fall on the same curve in Fig. 6 and Fig. 7 for short- and long-time cases, respectively. But it is noticed that the curves do not overlap for differing γ. This also means that the viscoelasticity cannot be neglected in the growth of bubbles in devolatilization conditions.

5. Summary

In this study the growth of vapor bubbles in upper con-

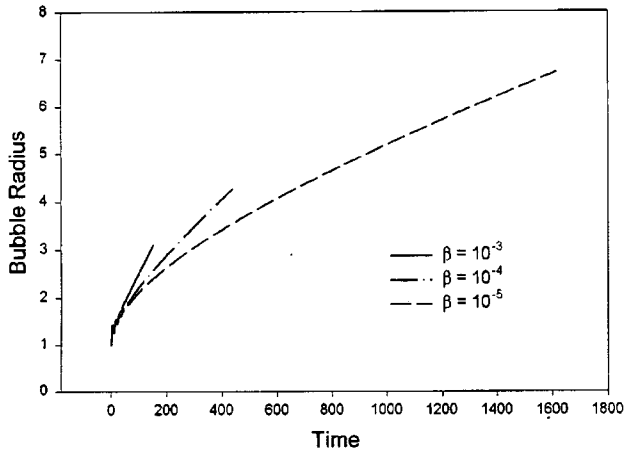

Fig. 3. The effect of β on bubble growth when Re = 0.1, De = 10, We = 0, γ = 1.

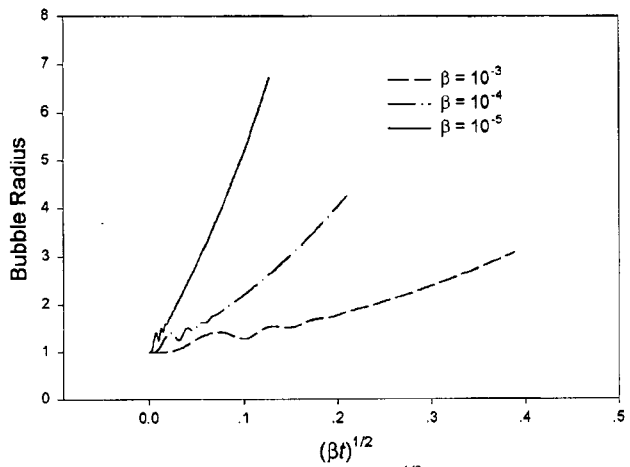

Fig. 4. Plot of bubble radius against $(\beta t)^{1/2}$ when Re = 0.1, De = 10, We = 0, γ = 1.

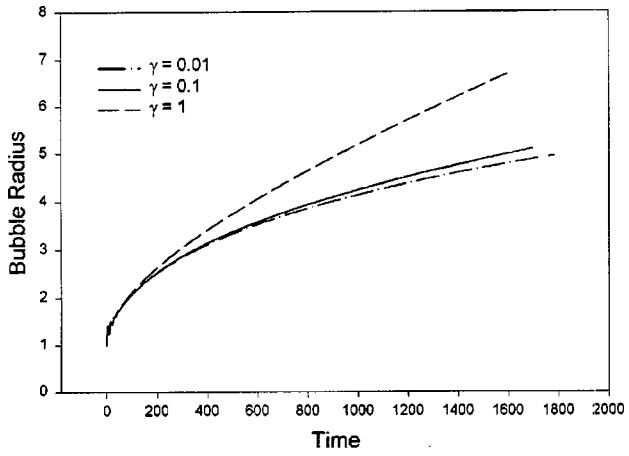

Fig. 5. The effect of γ on bubble growth when Re = 0.1, De = 10, We = 0 and $\beta = 10^{-5}$.

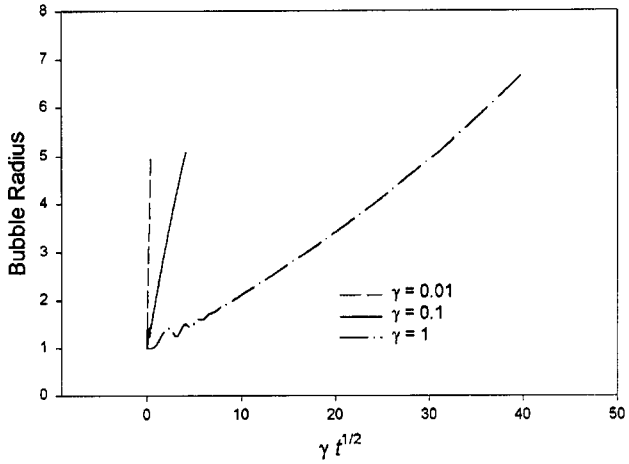

Fig. 6. Plot of bubble radius against $\gamma t^{1/2}$ when Re = 0.1, De = 10, We = 0 and $\beta = 10^{-5}$.

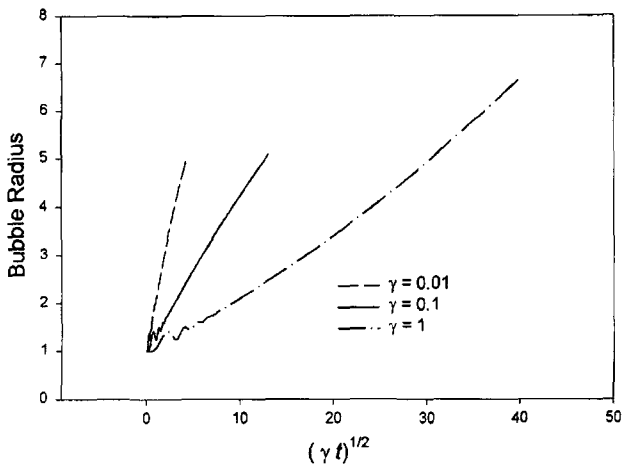

Fig. 7. Plot of bubble radius against $(\gamma t)^{1/2}$ when Re = 0.1, De = 10, We = 0 and $\beta = 10^{-5}$.

vected Maxwell fluid is theoretically investigated. Oscillatory behavior in bubble radius is observed during growth and the oscillatory behavior is found to be due to the interaction of mass transfer resistance and elasticity. It is found that the elasticity of fluid accelerates the growth and removal of volatile component. It is concluded that the bubble growth in the devolatilization of polymers is affected by both mass transfer resistance and viscoelasticity of fluids.

Acknowledgement

The author wishes to acknowledge the financial support by the Korea Research Foundation (Grant Number : 1997-001-E00467).

References

Afremanesh, A. and S.G. Advani, 1991, *Rheologica Acta* **30**, 274
Albalak, R.J., 1996, Polymer devolatilization, Marcel Dekker New York.
Biesenberger, J.A., 1983, Devolatilization of polymers, Hanser Munich.
Biesenberger, J.A. and D.H. Sebastian, 1983, Principles of polymer reaction engineering, Wiley, New York.
Doi, M. and S.F. Edwards, 1986, The theory of polymer dynamics, Clarendon Press, Oxford.
Duda, J.L., J.S. Vrentas, S.T. Ju and H.T. Liu, 1982, *AIChE J.* **28**, 279.
Favelukis, M. and R.J. Albalak, 1996, *Chem. Eng. J.* **63**, 149.
Han, C.D. and H.J. Yoo, 1981, *Polym. Eng. Sci.* **21**, 518.
Kim, C., 1994, *J. Non-Newt. Fluid Mech.* **55**, 37.
Mendelson, R.A., 1979, *J. Rheol.* **23**, 545.
Mendelson, R.A., 1980, *J. Rheol.* **24**, 765.
Papanastasiou, A.C., L.E. Scriven and C.W. Macosko, 1984, *J. Non-Newt. Fluid Mech.* **16**, 53.
Scriven, L.E., 1959, *Chem. Eng. Sci.* **10**, 1.
Venerus, D.C., N. Yala and B. Bernstein, 1998, *J. Non-Newt. Fluid Mech.* **75**, 55.
Vrentas, S.T. and J.L. Duda, 1977, *J. Polym. Sci. Part B: Polym. Phys.* **15**, 403 and 417.
Zana, E. and L.G. Leal, 1975, *Ind. Eng. Chem. Fund.* **10**, 54.